2950 Niles Road, St. Joseph, MI 49085-9659, USA
269.429.0300 fax 269.429.3852 hq@asabe.org www.asabe.org

An ASABE Meeting Presentation
DOI: https://doi.org/10.13031/aim.201800677
Paper Number: 1800677

3D computer vision and machine learning based technique for high throughput cotton boll mapping under field conditions

Shangpeng Sun[1], Changying Li[1], Andrew H. Paterson[2,3], Yu Jiang[1], Jon S. Robertson[2]

[1]School of Electrical and Computer Engineering, College of Engineering, University of Georgia, Athens, GA, United States

[2]Department of Crop and Soil Sciences, College of Agricultural and Environmental Sciences, University of Georgia, Athens, GA, United States

[3]Department of Genetics, Franklin College of Arts and Sciences, University of Georgia, Athens, GA, United States

Written for presentation at the
2018 ASABE Annual International Meeting
Sponsored by ASABE
Detroit, Michigan
July 29-August 1, 2018

ABSTRACT. *This study presented a multi-view imaging system with consumer-graded digital cameras to acquire images and reconstruct 3D model based on structure from motion principle in the field. A 3D point cloud data processing pipeline was proposed following three steps. First, the ground plane was removed using the RANSAC algorithm; then, a support vector machine based model was trained using color features for cotton boll segmentation from plants. At last, a 3D DBSCAN based method was developed to detect individual bolls from the segmented boll voxels. Experiments with cotton plots showed that good quality 3D model can be reconstructed and the proposed 3D boll mapping methods achieved an accuracy of around 90%, and the squared Pearson correlation was 0.95 between the sensor measurement and the ground truth. The system not only successfully estimated the total number of cotton bolls, but also provided location information for each individual bolls. This was a significant contribution compared to 2D image based methods. The 3D boll mapping information was useful for monitoring crop growth and yield prediction.*

Keywords. *3D cotton boll mapping, computer vison, point cloud, structure from motion, support vector machine*

Introduction

Cotton is considered to be among the most economically important crops, with 25% fiber production used throughout the world. In 2017, an estimated 12 million acres of cotton crops were grown in the US, resulting in a value of $21 billion for the US cotton industry (USDA, 2017). Yield prediction is important for growers and researchers. The information supports growers to make timely decisions on crop management such as harvest labor requirement and storage arrangement, thereby preventing yield loss and reducing cost, and plays an important role on evaluation of crop growth conditions and cultivation practices. However, traditional yield estimation based on manual sampling method is labor

intensive, time consuming and prone to be inaccurate. Computer vision based systems using agriculture robots (Oberti and Shapiro, 2016) or unmanned aerial vehicles (UAV) (Xu et al., 2017) provided several advantages for crop growth monitoring and yield estimation such as efficiency improvement and human error reduction (Qureshi et al., 2017).

2D image based methods have been widely used for fruit detection in various crops (Gongal et al., 2015). In terms of cotton, Li et al. (2016) applied a region-based semantic segmentation algorithm to recognize cotton bolls in RGB images. Two digital cameras were used to capture images every an hour in the field, one was from downward view at a height of 5 m, and the other from forward view at a height of 0.3 m. For image processing, first, simple linear iterative clustering (SLIC) algorithm was used to extract superpixels for each image; then a 110-dimensional feature vector for each superpixel was built including color and texture features. A random forest (RF) model was trained for segmentation of cotton bolls and background including foliage, branches, sky and plastic. The average accuracy reported in the study was 99.4%, which outperformed several other similar studies such as the HSV-T based method (Jie-ding et al., 2008), the YCbCr-FV based method (Liu et al., 2011) and OHTA-SVM based method (Chen et al., 2013). The study focused on boll recognition, which could be used to provide boll opening stage information. However, individual boll counting was not explored in the study. In addition, there existed significant drawbacks for 2D image based fruit detection. Occlusion is a big issue for plant phenotyping, especially under field conditions. 2D image will cause more occlusion problems due to the lack of depth information. Although several different methods were proposed to address this problem, it remains unresolved.

To address the shortcomings of 2D image based methods, much effort was made on the development of 3D imaging systems for agriculture applications in the past decade (Gongal et al., 2015). Though there are many ways for 3D scanning and reconstruction, Time-of-Flight (ToF) and triangulation are the two most used technologies in agriculture applications. ToF systems estimate the true distance from the sensor to the object based on the flight time of an emitted signal which hits the object and returns to the receiver. Triangulation techniques measure distances based on a triangle consisting of the target and two different sensors. To compute the distance, the two sensors need to be calibrated with respect to each other. The commonly used sensors based on ToF principle include LiDAR and Kinect V2; while techniques based on triangulation principle include stereo vision and structure from motion (SfM). Sun et al. (2018) applied a 2D LiDAR to generate 3D models of cotton plants with a top-down view in field conditions, and then developed algorithms for calculating morphological traits including canopy height, projected canopy area and plant volume. Based on the results, the plant growth model was built and the correlation between morphological traits and yield was analyzed. However, since the resolution of the point cloud was not high enough and lack color information, organ-level detailed traits such as leaf angle could not be extracted using the sensor. LiDAR technologies were also commonly used in other applications such as plant height (Sun et al., 2017) and leaf area index (LAI) estimation (Pearse et al., 2016). Tao and Zhou (2017) applied a Kinect V2 sensor to capture 3D point cloud in an apple orchard, and developed an apple recognition method based on color region growth segmentation and support vector machine (SVM). The best reported accuracy was up to 92.3%. However, one major limitation of the study was that the performance of color region growth method could decrease due to varied illumination conditions in the field, which played negative influence for apple recognition. Jiang et al. (2018) developed a ground mobile system for field based phenotyping and a Kinect V2 sensor (Jiang et al., 2017) was used for quantitative analysis of cotton canopy size for the whole growing season. Fernandez et al. (2017) developed a field-based platform for high through phenotyping of tall biomass crops with stereo RGB cameras, from which the plant height and stem diameter can be extracted. Nguyen et al. (2016) developed a field-based system with 32 cameras for plant 3D reconstruction. Although good quality 3D models can be obtained, one major limitation was that the system was only suitable for the condition that single small sized plants, which limited its applications.

In this study, we proposed a novel 3D computer vision and machine learning based system for cotton boll mapping. Compared to the study conducted by Li et al. (2017) with 2D images, one of main contributions of this study was that not only boll segmentation was implemented, but individual bolls were detected, from which the information of total number of bolls and location of each boll can be obtained. In addition, cotton plants have what some suggest to be most complex structure of all major field crops (Mauney, 1986). Cotton bolls have varied and complex shapes, especially the opened bolls could be drooped when they are fully opened, resulting in serious occlusion issue compared to other fruits with a rigid shape such as apples. Therefore, new detection methods were needed to detect individual bolls.

The overall goal of this study was to develop a system for 3D cotton boll mapping. Specific objectives were to (1) implement a prototype platform for image acquisition using multiple cameras in the field for 3D reconstruction; (2) develop an automated boll segmentation and mapping algorithm; (3) validate the performance of the proposed method compared to the ground truth.

Material and Methods

Experimental field and plant material

The experimental field was located at Iron Horse Farm (IHF) in Greene County, GA, USA (Figure 1). For each row, there were 19 plots which was around 3.05 m long. A total of 10 plots were imaged on Dec 14, 2017. The ground truth of

boll number for each plot was manually counted, ranging from 85 to 311.

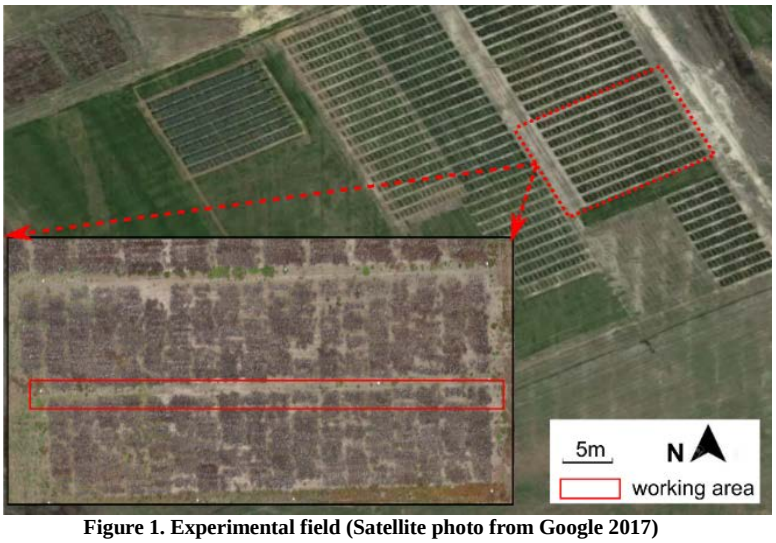

Figure 1. Experimental field (Satellite photo from Google 2017)

Multi-view image acquisition and 3D reconstruction

Five digital cameras (Fujifilm X-A10, Fujifilm Holdings Corporation, NY, USA), which captured images of cotton plants from side and top perspectives, were mounted on a tractor (Spider DL, LeeAgra, Inc., Lubbock, TX, USA) (Figure 2a and b). Camera C5 was mounted at a height of around 2 m, capturing images from top-down view. The other four cameras scanned plants from side view. Camera C1 and C2 were at the same height of around 0.3 m, and camera C3 and C4 were also at the same height with a value of around 0.8 m. Since the four cameras were mounted at the same side, the tractor should be driven two runs for each plot as indicated in Figure 2a with red arrows in order to ensure that both sides of plants were scanned. Figure 1c presented an example of the camera positions for a plot. When capturing images, cameras were configured to be shutter speed priority model with a shutter speed of 1/200 s, 16 mm focal length and 200 ISO. Images were stored in JPG format with a resolution of 4896×3264.

After image acquisition was finished, 3D reconstruction was implemented based on SfM by software Agisoft PhotoScan. An example of reconstructed 3D model of one plot cotton plants was showed in Figure 2d.

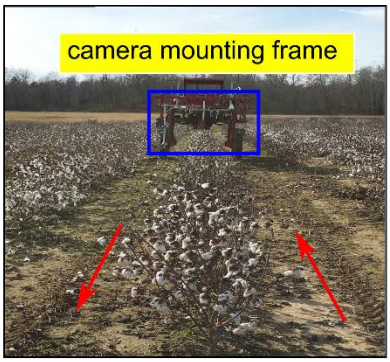

(a) platform for image acquisition

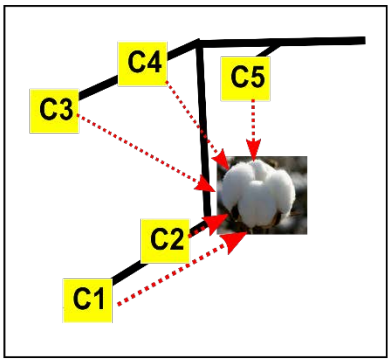

(b) layout of cameras

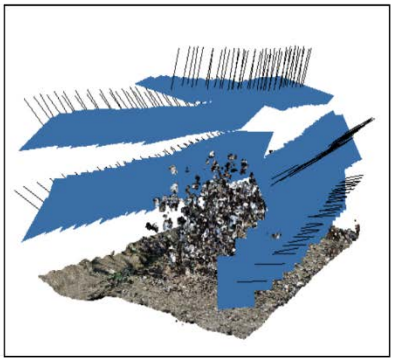

(c) camera position for the image set

(d) reconstructed 3D point cloud

Figure 2. Image acquisition platform and example of reconstructed 3D model of cotton plants based on structure from motion using multiple view digital images. (a) A tractor platform was used to collect data in the field. (b) Layout of the five cameras. (c) Example of camera positions for a reconstructed 3D model. (d) An example of reconstructed 3D model.

Algorithm for 3D Boll mapping

Image processing pipeline for 3D boll mapping was presented in Figure 3. First, RANSAC algorithm was applied on the original point cloud (Figure 3a) to remove the ground plane, resulting that point cloud of plant was obtained (Figure 3b); then, a SVM-based model was trained based on color features to separate cotton bolls and branches (Figure 3c); after that a 3D DBSCAN based algorithm was developed to extract individual bolls. Each boll was indicated using a bounding box with red color (Figure 3d).

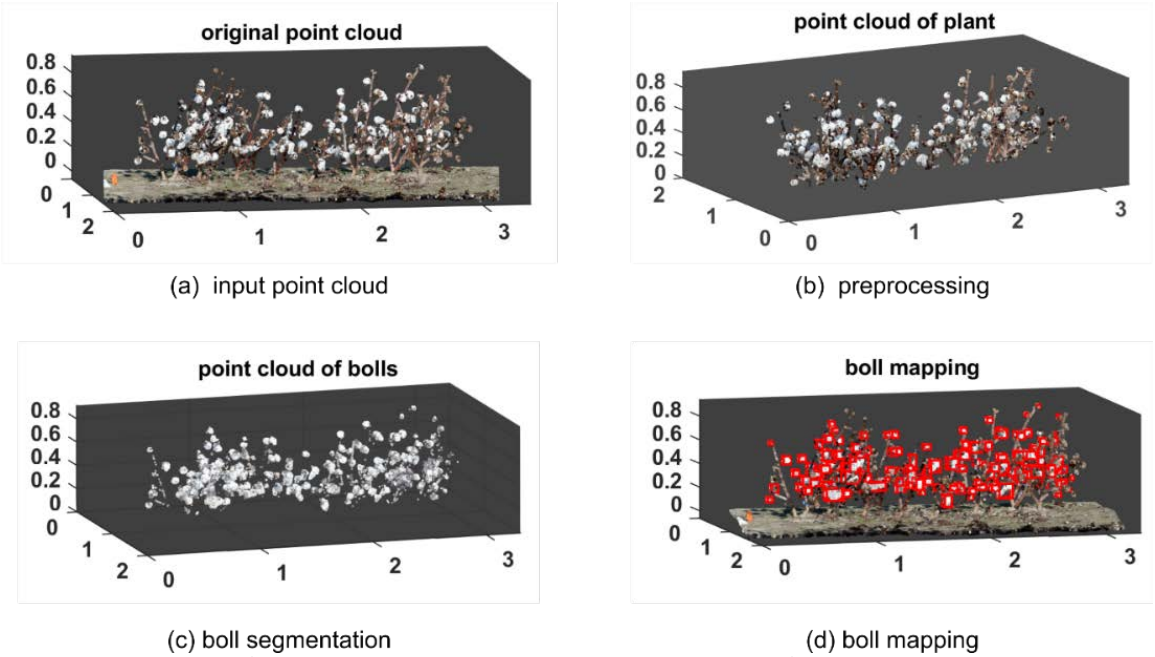

Figure 3. Data processing pipeline for 3D boll mapping. (a) Original point cloud used as input for the proposed algorithm; (b) RANSAC based method was used to remove the ground plane; (3) A SVM-based model was trained to segment boll voxels; (4) 3D DBSCAN-based method was used for 3D boll mapping.

After the ground plane was removed from the original point cloud, only two categories of items—bolls and branches—were left. Based on the observation, a significant difference existed for voxels between bolls and branch in terms of color features. Therefore, color information was selected for point cloud segmentation. In this study, a support vector machine (SVM) model was trained as the classifier. The training and testing datasets were manually labeled in 2D images. a SLIC based labeling method was developed in order to improve sample labeling accuracy and efficiency. First, patches including bolls and branches under sunlight and shadow illumination conditions were extracted from original images; then SLIC was applied on each patch to generate superpixels (Figure 4). For each superpixel, the average intensity was calculated and an 8-dimension feature vector was built, consisting of (R/B - R/G), (R/B - B/G), (R/G - G/B) in RGB color space, L, a in CIELab color space, H, S in HSV color space, and Y in YCbCr color space. A SVM model was trained with linear kernel function with default configuration based on LIBSVM package.

Figure 4. SLIC-based sample labeling method. Representative patches including bolls and branches were extracted from original images, and then superpixels were generated using simple linear iterative clustering algorithm.

Once the point cloud of boll voxels was obtained, a 3D DBSABN based clustering algorithm was applied to detect individual bolls based on the voxel density and boll size features (Figure 5). First, 3D DBSCAB was applied on the boll voxels to obtain clusters of voxels (potential bolls); then, a size filter was used to remove noise clusters. To do this, a unit volume V_{unit} was established based on the size of real bolls. A boll was assumed to be a sphere. In this study, let V_{unit} equal to the volume of a sphere with a dimeter of 6 cm based on the manual measurements of the diameter for 20 samples. For each cluster from 3D DBSCAN, the volume was calculated using convex hull method. If the volume was less than 0.1 V_{unit}, the cluster was considered to be noise; if the volume was between 0.1 V_{unit} and 2 V_{unit}, the cluster was considered to

be an individual boll; if the volume was greater than 2 V_{unit}, the cluster would be divided to several sub-clusters since this large cluster could be consisted by several connected bolls. The number of the sub-clusters was computed using eq (1).

$$k = \Phi\left(V_i \Big/ V_{unit}\right) \tag{1}$$

Where, V_i was the volume of cluster i, Φ was a function which mapped a real number to the least succeeding integer, k was the splitting number.

Algorithm: Individual boll detection

```
Require: pt        # point cloud of boll voxels
Require: V_unit    # the unit volume used as a size filter
C ← Ω(pt)          # Ω: 3D DBSCAN function
V ← Ψ(C)           # Ψ: convex hull based volume calculation function
B ← 0              # initialize boll number
for i = 1 to size(C)
    switch V_i
        case: 0.1V_unit < V(i) < 2V_unit
            B ← B+1
        case: V_i > 2V_unit
            k ← Φ(V_i / V_unit)
            B ← B + k
        otherwise:
            B ← B
    end switch
end for
Return B
```

Figure 5. Algorithm for individual boll detection

Validation methodology

In order to validate the performance of the proposed boll mapping algorithm, the mean absolute percentage error E_s was computed between the sensor measured boll numbers B_i and the manual measurements m_i by applying eq (2). N was the number of plots.

$$E_s = \frac{100 \times \sum_{i=1}^{N} \left|B_i - m_i\right| \Big/ m_i}{N} \tag{2}$$

In addition, to be able to test the correlation between the sensor measurements and the ground truth, the coefficient of determination (R^2) and the root mean square errors (RMSE) were calculated. The R^2 value were to 1, the stronger the correlation between two measurements.

Resutls and Discussion

System layout and 3D reconstruction from multi-view images

High quality 3D reconstruction played a significant role for cotton boll mapping, which requested a reliable and efficient data collection system (Dong et al., 2016). In this study, we demonstrated a multi-view camera system for image acquisition in the field with consumer-grade cameras and the 3D reconstruction with SfM-based software Agisoft PhotoScan shown as in Figure 2. Although relatively good quality 3D models were obtained, there was significant room for system improvement. For the current system, four cameras were mounted at the same side. Although this one-side setup avoided the problem that a camera at one side could capture another camera at the other side for two-sides setup, the tractor had to move two runs in order to scan both sides of cotton plants, limiting the throughput capability. Therefore, one of the future work is to explore the two-sides setup in order to double the data collection efficiency, which is particularly useful for large field applications. Varied illumination condition in the field was detrimental for 3D model reconstruction. One solution is to add an enclosure to provide a consistent illumination environment.

Semantic segmentation of boll voxels

A total of 1050 samples were manually labeled including 543 boll instances and 507 branch instances. The whole dataset was divided into training and testing subsets with a ratio of 7:3. A SVM model was trained with linear kernel function with the testing accuracy 97.2%. Overall, the obtained SVM classifier had a good performance for boll segmentation from branch, although there existed false positive (FP) and false negative (FN) voxels. A representative result was demonstrated in Figure 6, in which boll voxels detected by the SVM classifier were indicated by red color. The FP voxels were caused by branch components under strong sunlight, since the components presented similar color features to bolls voxels. Since FP voxels would result in overestimation of the total boll numbers, several methods were applied to remove them during boll mapping operation. Regarding FN voxels, which were mainly caused due to shadow effects. If just part of a boll, not all boll voxels, were misclassified, the boll detection algorithm had a great of potential to correctly recognize them as an individual boll.

In this study, semantic segmentation of boll voxels was conducted on individual voxel level based on color features. However, more 3D feature describers such as shape (Rusu, 2010), Fast Point Feature Histogram (FPFH) (Rusu et al., 2009) and spectral features (Munoz et al., 2009), which were independent on illumination condition, could be used if supervoxels were generated for the point cloud (Papon et al., 2013). In addition, the computational cost could be reduced with supervoxel-based methods.

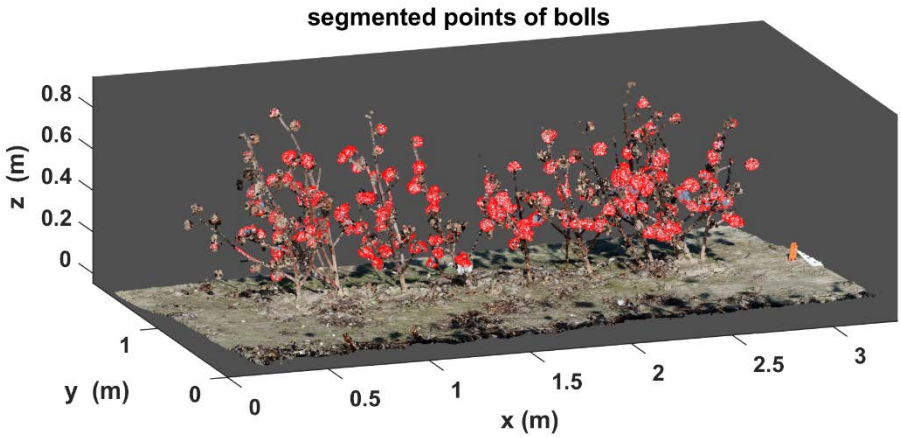

Figure 6. Representative results of semantic segmentation of cotton boll voxels

3D boll mapping

The proposed individual boll detection method, which was implemented based on 3D point cloud, reduced the challenge of boll occlusion issue compared to studies using 2D image based methods (Malik et al., 2016; Stein et al., 2016; Wang et al., 2016; Bargoti and Underwood, 2017). A representative result was presented in Figure 7, in which 177 bolls were detected while the ground truth was 192. In Figure 7, all individual bolls, which were spread apart and appeared without occlusions in the point cloud, were successfully detected. The depth and the size information made significant contribution on the splitting operation for clusters in which several bolls were connected, although the method might not extract the exact number of individual bolls from the clusters.

Statistical analysis also indicated that sufficient accuracy was achieved (Figure 8). The mean absolute percentage error was around 9.75%, with a standard deviation of 0.14, which was better than fruit detection studies in (Stein et al., 2016; Wang et al., 2016; Bargoti and Underwood, 2017) using 2D images. The squared Pearson correlation (R^2 = 0.95) between sensor and manual measurements showed strong correlations as it approached 1, and with the root mean square error of RMSE = 13.49.

It has potential to further improve the performance when more features and advanced algorithms were applied (Hackel et al., 2017; Qi et al., 2017; Verdoja et al., 2017). Another important factor influencing boll mapping performance was the time window of image acquisition. Compared to fruits with rigid shapes such as apples and citrus, cotton bolls would be drooped when they were fully opened, which resulted in worse situations in terms of boll connection. Therefore, image acquisition will be conducted before bolls are drooped in the future.

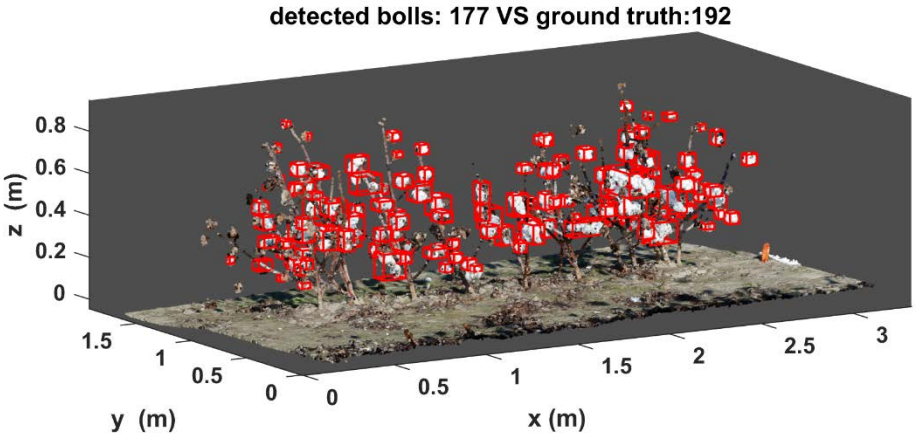

Figure 7. Representative results of 3D boll mapping.

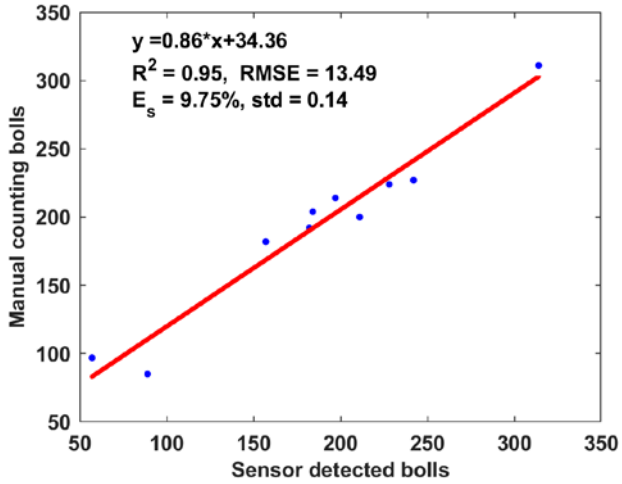

Figure 8. Correlation analysis results between sensor measurements and the ground truth.

Yield prediction

Overall, the boll number showed a good correlation with yield, with the R^2 value between manual measurements and yield was 0.74, and between sensor measurements and yield was 0.83 (Figure 9). If more information was included such as volume of each boll and fiber density, it can be concluded that better correlation can be achieved.

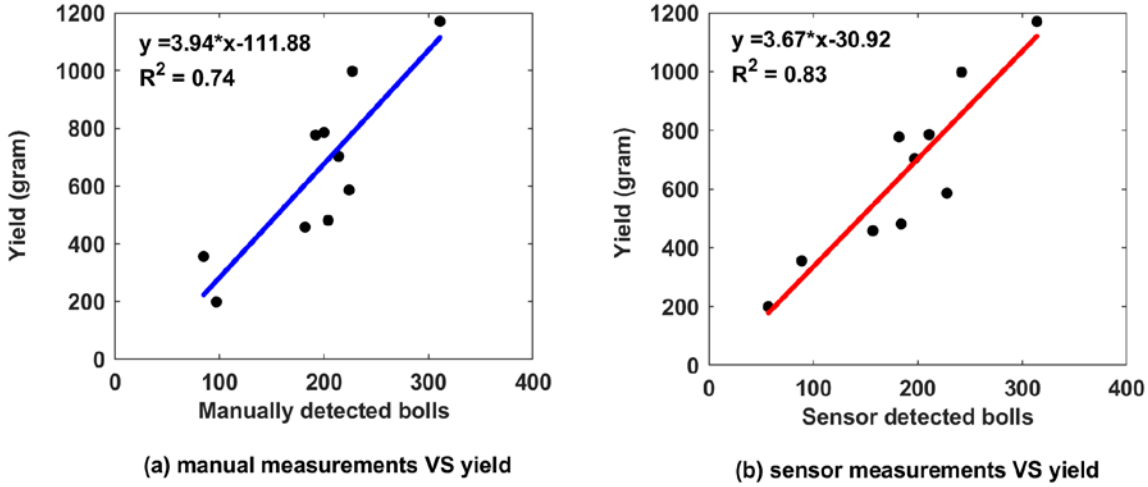

Figure 9. Comparison of correlation analysis between boll numbers and yield. (a) correlation between manual measurements and yield; (b) correlation between sensor measurements and yield.

Conclusion

The demonstrated multi-view camera system with structure from motion based method had the potential to acquire colored 3D point cloud of cotton plants in the field. The efficiency of the data collection system could be improved when applying two-side setup with more cameras. Moreover, higher quality raw images could be obtained if an enclosure is added since it provides consistent illumination environment. The proposed 3D cotton boll mapping method achieved a better performance than similar studies using 2D image-based methods. In addition, it provided the location information for each boll, which is a significant contribution of this study. In the future, efforts will be made on both the data collection system and point cloud processing methods.

Acknowledgements

The authors gratefully thank Tariq Shehzad, Jeevan Adhikari, Rui Xu, Mengyun Zhang and Lujun Li for their assistance in conducting the experiments and the ground truth data measurements. The authors thank Kyle Hunady for his assistance in sample labeling.

References

Bargoti, S., and Underwood, J.P. (2017). Image segmentation for fruit detection and yield estimation in apple orchards. *Journal of Field Robotics*.

Chen, Q., Lai, H., Wang, X., Ren, L., and Liu, J. (2013). An cotton image segmentation algorithm based on support vector machine. *Comput. Eng* 39**,** 266-269.

Dong, J., Burnham, J.G., Boots, B., Rains, G.C., and Dellaert, F. (2016). 4D Crop Monitoring: Spatio-Temporal Reconstruction for Agriculture. *arXiv preprint arXiv:1610.02482*.

Fernandez, M.G.S., Bao, Y., Tang, L., and Schnable, P.S. (2017). A High-Throughput, Field-Based Phenotyping Technology for Tall Biomass Crops. *Plant Physiology* 174(4)**,** 2008-2022. doi: 10.1104/pp.17.00707.

Gongal, A., Amatya, S., Karkee, M., Zhang, Q., and Lewis, K. (2015). Sensors and systems for fruit detection and localization: A review. *Computers and Electronics in Agriculture* 116**,** 8-19.

Hackel, T., Savinov, N., Ladicky, L., Wegner, J.D., Schindler, K., and Pollefeys, M. (2017). Semantic3D. net: A new large-scale point cloud classification benchmark. *arXiv preprint arXiv:1704.03847*.

Jiang, Y., Li, C., Paterson, A., Sun, S., Xu, R., and Robertson, J. (2017). Quantitative analysis of cotton canopy size in field conditions using a consumer-grade RGB-D camera. *Frontiers in plant science* 8**,** 2233.

Jiang, Y., Li, C., Robertson, J.S., Sun, S., Xu, R., and Paterson, A.H. (2018). GPhenoVision: A Ground Mobile System with Multi-modal Imaging for Field-based High Throughput Phenotyping of Cotton. *Scientific reports* 8(1)**,** 1213.

Jie-ding, W., Shu-min, F., Mu-lan, W., and Jian-ning, Y. (2008). Research on the Segmentation Strategy of the Cotton Images on the Natural Condition Based upon the HSV Color-Space Model. *Cotton Science* 1**,** 010.

Li, Y., Cao, Z., Lu, H., Xiao, Y., Zhu, Y., and Cremers, A.B. (2016). In-field cotton detection via region-based semantic image segmentation. *Computers and Electronics in Agriculture* 127**,** 475-486. doi: http://dx.doi.org/10.1016/j.compag.2016.07.006.

Li, Y., Cao, Z., Xiao, Y., and Cremers, A.B. (2017). DeepCotton: in-field cotton segmentation using deep fully convolutional network. *Journal of Electronic Imaging* 26(5)**,** 053028.

Liu, J.-S., Lai, H.-C., and Jia, Z.-H. (2011). Image segmentation of cotton based on YCbCcr color space and fisher discrimination analysis. *Acta Agronomica Sinica* 33(7)**,** 1274-1279. doi: 10.3724/SP.J.1006.2011.01274.

Malik, Z., Ziauddin, S., Shahid, A.R., and Safi, A. (2016). Detection and Counting of On-Tree Citrus Fruit for Crop Yield Estimation. *International Journal of Advanced Computer Science and Applications* 7(5)**,** 519-523.

Mauney, J.R. (1986). *Vegetative growth and development of fruiting sites.*

Munoz, D., Vandapel, N., and Hebert, M. (Year). "Onboard contextual classification of 3-d point clouds with learned high-order markov random fields", in: *Robotics and Automation, 2009. ICRA'09. IEEE International Conference on*: IEEE).

Nguyen, T.T., Slaughter, D.C., Townsley, B., Carriedo, L., Julin, N., and Sinha, N. (Year). "Comparison of structure-from-motion and stereo vision techniques for full in-field 3d reconstruction and phenotyping of plants: An investigation in sunflower", in: *2016 ASABE Annual International Meeting*: American Society of Agricultural and Biological Engineers).

Oberti, R., and Shapiro, A. (2016). Advances in robotic agriculture for crops. *Biosystems Engineering* 146**,** 1-2. doi: http://dx.doi.org/10.1016/j.biosystemseng.2016.05.010.

Papon, J., Abramov, A., Schoeler, M., and Wörgötter, F. (Year). "Voxel cloud connectivity segmentation-supervoxels for point clouds", in: *Computer Vision and Pattern Recognition (CVPR), 2013 IEEE Conference on*: IEEE), 2027-2034.

Pearse, G.D., Watt, M.S., and Morgenroth, J. (2016). Comparison of optical LAI measurements under diffuse and clear skies after correcting for scattered radiation. *Agricultural and Forest Meteorology* 221**,** 61-70. doi: http://dx.doi.org/10.1016/j.agrformet.2016.02.001.

Qi, C.R., Yi, L., Su, H., and Guibas, L.J. (Year). "Pointnet++: Deep hierarchical feature learning on point sets in a metric

space", in: *Advances in Neural Information Processing Systems*), 5105-5114.
Qureshi, W.S., Payne, A., Walsh, K.B., Linker, R., Cohen, O., and Dailey, M.N. (2017). Machine vision for counting fruit on mango tree canopies. *Precision Agriculture* 18(2)**,** 224-244. doi: 10.1007/s11119-016-9458-5.
Rusu, R.B. (2010). Semantic 3D object maps for everyday manipulation in human living environments. *KI-Künstliche Intelligenz* 24(4)**,** 345-348.
Rusu, R.B., Blodow, N., and Beetz, M. (Year). "Fast point feature histograms (FPFH) for 3D registration", in: *Robotics and Automation, 2009. ICRA'09. IEEE International Conference on*: IEEE), 3212-3217.
Stein, M., Bargoti, S., and Underwood, J. (2016). Image Based Mango Fruit Detection, Localisation and Yield Estimation Using Multiple View Geometry. *Sensors* 16(11)**,** 1915.
Sun, S., Li, C., Paterson, A., Jiang, Y., Xu, R., Robertson, J., et al. (2018). In-field high throughput phenotyping and cotton plant growth analysis using LiDAR. *Frontiers in Plant Science* 9**,** 16.
Sun, S., Li, C., and Paterson, A.H. (2017). In-Field High-Throughput Phenotyping of Cotton Plant Height Using LiDAR. *Remote Sensing* 9(4)**,** 377.
Tao, Y., and Zhou, J. (2017). Automatic apple recognition based on the fusion of color and 3D feature for robotic fruit picking. *Computers and Electronics in Agriculture* 142**,** 388-396.
USDA (2017). https://www.fas.usda.gov/data/cotton-world-markets-and-trade.
Verdoja, F., Thomas, D., and Sugimoto, A. (Year). "Fast 3D point cloud segmentation using supervoxels with geometry and color for 3D scene understanding", in: *Multimedia and Expo (ICME), 2017 IEEE International Conference on*: IEEE), 1285-1290.
Wang, C.L., Zou, X.J., Tang, Y.C., Luo, L.F., and Feng, W.X. (2016). Localisation of litchi in an unstructured environment using binocular stereo vision. *Biosystems Engineering* 145**,** 39-51. doi: 10.1016/j.biosystemseng.2016.02.004.
Xu, R., Li, C., Paterson, A., Jiang, Y., Sun, S., and Robertson, J. (2017). Cotton bloom detection using aerial images and convolutional neural network. *Frontiers in Plant Science* 8**,** 2235.